



# Room-temperature multiferroic behavior in layer-structured Aurivillius phase ceramics

Cite as: Appl. Phys. Lett. **117**, 052903 (2020); <https://doi.org/10.1063/5.0017781>

Submitted: 09 June 2020 . Accepted: 25 July 2020 . Published Online: 07 August 2020

Zheng Li, Vladimir Koval , Amit Mahajan, Zhipeng Gao, Carlo Vecchini, Mark Stewart, Markys G. Cain , Kun Tao, Chenglong Jia , Giuseppe Viola, and Haixue Yan 



View Online



Export Citation



CrossMark

## ARTICLES YOU MAY BE INTERESTED IN

[Intrinsic piezoelectricity in \(K,Na\)NbO<sub>3</sub>-based lead-free single crystal: Piezoelectric anisotropy and its evolution with temperature](#)

Applied Physics Letters **117**, 052904 (2020); <https://doi.org/10.1063/5.0012124>

[Current-induced bulk magnetization of a chiral crystal CrNb<sub>3</sub>S<sub>6</sub>](#)

Applied Physics Letters **117**, 052408 (2020); <https://doi.org/10.1063/5.0017882>

[Magnetic transition behavior and large topological Hall effect in hexagonal Mn<sub>2-x</sub>Fe<sub>1+x</sub>Sn \(x = 0.1\) magnet](#)

Applied Physics Letters **117**, 052407 (2020); <https://doi.org/10.1063/5.0011570>



**Measure Ready**  
**FastHall™ Station**

The highest performance tablet system...  
for van der Pauw and Hall bar samples

[Learn more](#)

Lake Shore  
CRYOTRONICS



BLFC  $B_{5.25}La_{0.75}Fe_{1-x}Co_xO_{18}$  (P)  $a = 5.4530(2)$  Å,  $b = 5.4427(1)$  Å,  $c = 50.670(2)$  Å,  $V = 1503.6(1)$  Å<sup>3</sup>,  $Z = 4$ ,  $FWM = 0.17$  (111),  $0.19$  (111),  $0.21$  (111),  $0.22$  (111),  $0.23$  (111),  $0.24$  (111),  $0.25$  (111),  $0.26$  (111),  $0.27$  (111),  $0.28$  (111),  $0.29$  (111),  $0.30$  (111),  $0.31$  (111),  $0.32$  (111),  $0.33$  (111),  $0.34$  (111),  $0.35$  (111),  $0.36$  (111),  $0.37$  (111),  $0.38$  (111),  $0.39$  (111),  $0.40$  (111),  $0.41$  (111),  $0.42$  (111),  $0.43$  (111),  $0.44$  (111),  $0.45$  (111),  $0.46$  (111),  $0.47$  (111),  $0.48$  (111),  $0.49$  (111),  $0.50$  (111),  $0.51$  (111),  $0.52$  (111),  $0.53$  (111),  $0.54$  (111),  $0.55$  (111),  $0.56$  (111),  $0.57$  (111),  $0.58$  (111),  $0.59$  (111),  $0.60$  (111),  $0.61$  (111),  $0.62$  (111),  $0.63$  (111),  $0.64$  (111),  $0.65$  (111),  $0.66$  (111),  $0.67$  (111),  $0.68$  (111),  $0.69$  (111),  $0.70$  (111),  $0.71$  (111),  $0.72$  (111),  $0.73$  (111),  $0.74$  (111),  $0.75$  (111),  $0.76$  (111),  $0.77$  (111),  $0.78$  (111),  $0.79$  (111),  $0.80$  (111),  $0.81$  (111),  $0.82$  (111),  $0.83$  (111),  $0.84$  (111),  $0.85$  (111),  $0.86$  (111),  $0.87$  (111),  $0.88$  (111),  $0.89$  (111),  $0.90$  (111),  $0.91$  (111),  $0.92$  (111),  $0.93$  (111),  $0.94$  (111),  $0.95$  (111),  $0.96$  (111),  $0.97$  (111),  $0.98$  (111),  $0.99$  (111),  $1.00$  (111).

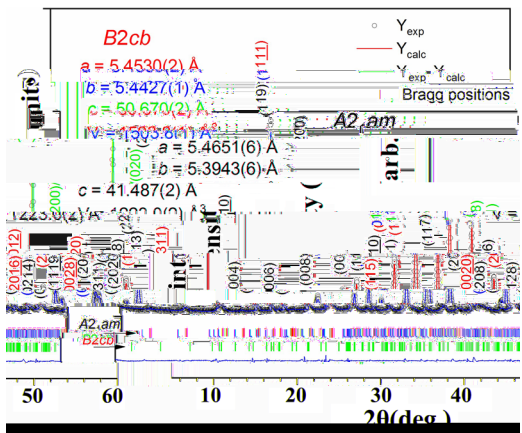


FIG. 1. XRD patterns of B2cb and A2am phases.

BLFC  $B_{5.25}La_{0.75}Fe_{1-x}Co_xO_{18}$  (P)  $a = 5.4530(2)$  Å,  $b = 5.4427(1)$  Å,  $c = 50.670(2)$  Å,  $V = 1503.6(1)$  Å<sup>3</sup>,  $Z = 4$ ,  $FWM = 0.17$  (111),  $0.19$  (111),  $0.21$  (111),  $0.22$  (111),  $0.23$  (111),  $0.24$  (111),  $0.25$  (111),  $0.26$  (111),  $0.27$  (111),  $0.28$  (111),  $0.29$  (111),  $0.30$  (111),  $0.31$  (111),  $0.32$  (111),  $0.33$  (111),  $0.34$  (111),  $0.35$  (111),  $0.36$  (111),  $0.37$  (111),  $0.38$  (111),  $0.39$  (111),  $0.40$  (111),  $0.41$  (111),  $0.42$  (111),  $0.43$  (111),  $0.44$  (111),  $0.45$  (111),  $0.46$  (111),  $0.47$  (111),  $0.48$  (111),  $0.49$  (111),  $0.50$  (111),  $0.51$  (111),  $0.52$  (111),  $0.53$  (111),  $0.54$  (111),  $0.55$  (111),  $0.56$  (111),  $0.57$  (111),  $0.58$  (111),  $0.59$  (111),  $0.60$  (111),  $0.61$  (111),  $0.62$  (111),  $0.63$  (111),  $0.64$  (111),  $0.65$  (111),  $0.66$  (111),  $0.67$  (111),  $0.68$  (111),  $0.69$  (111),  $0.70$  (111),  $0.71$  (111),  $0.72$  (111),  $0.73$  (111),  $0.74$  (111),  $0.75$  (111),  $0.76$  (111),  $0.77$  (111),  $0.78$  (111),  $0.79$  (111),  $0.80$  (111),  $0.81$  (111),  $0.82$  (111),  $0.83$  (111),  $0.84$  (111),  $0.85$  (111),  $0.86$  (111),  $0.87$  (111),  $0.88$  (111),  $0.89$  (111),  $0.90$  (111),  $0.91$  (111),  $0.92$  (111),  $0.93$  (111),  $0.94$  (111),  $0.95$  (111),  $0.96$  (111),  $0.97$  (111),  $0.98$  (111),  $0.99$  (111),  $1.00$  (111).

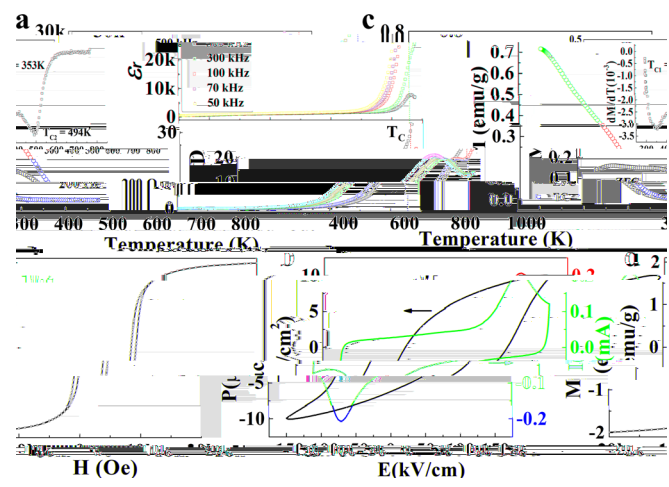


FIG. 2. Temperature dependence of magnetic and ferroelectric properties.

$\sim 494$  K (M/),  
 $B_6FC_3O_{18}$  (526 K).<sup>23</sup>  
 BLFC  
 $F^{3+}$ ,  $O$ ,  $F^{3+}$ ,  $C^{3+}$ ,  $O$ ,  $C^{3+}$ ,  $F^{3+}$ ,  $O$ ,  $C^{3+}$  ( ).<sup>24</sup>  
 ED  
 $\sim 353$  K  
 $C_2F_4O_4$  (460 K) (M)  $C_2F_4O_4$  (16,25)  
 $16.235 / .25$ ,  $0.22$   $0.32 /$ ,  $1.4$  .%  
 $C_2F_4O_4$  BLFC  
 $M = 1.85 /$ ,  $F . 2( ) . I$   
 $M H$   
 $2 (F . 3)$   
 $425$  K  $1.58 /$   $0.27 /$ , ED  
 BLFC  
 $F . 3$   
 $F^{3+}$ ,  $O$ ,  $C^{3+}$   
 (DF)  $ab initio$   
 (A P)  
 $F = 2$   $C = 3$   $F$   $C$ ,  
 (GGA)  $I$   
 BLFC  
 $F . 3(a)$ ,  $F^{3+}$   $C^{3+}$  ( $3.1$   $2.1 \mu_B/a$ ),  
 $0.1 \mu_B/a$ .  
 $F O_6$   $C O_6$   
 $F / C$   $F . 3( )$ .  
 $F^{3+}$   $C^{3+}$   
 $( . , )$   $( . , )$   
 $E_{FM} - E_{AFM} = -144.1$ .  
 $H$  (FM)  $43.5$  ( $504.6$  K), FM  
 $1$  FC/FC  $F . 2( )$ .  
 $a b$   
 $010$   
 $F . 4$   
 BLFC  $I$   
 $399$  O  $F .$   
 $5( ) . A$   $P F M$  BLFC  $F$

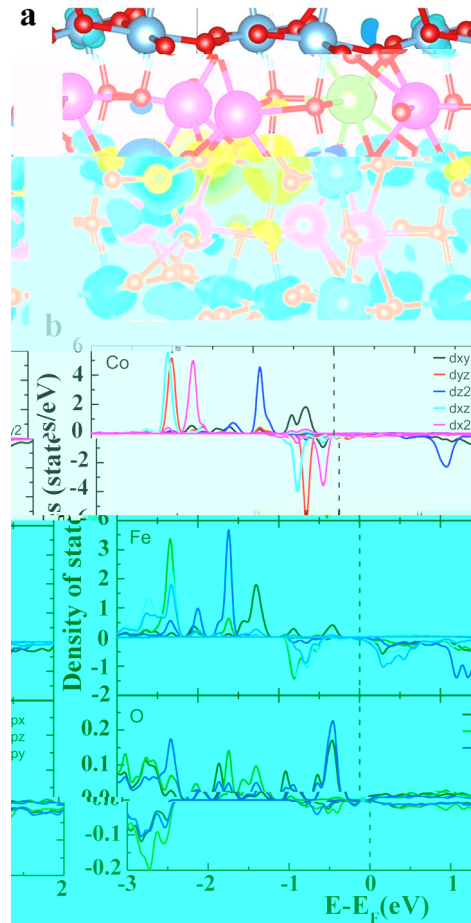


FIG. 3. (a) Crystal structure of BLFC. (b) Density of states (DOS) for Co, Fe, and O ions. The DOS is calculated using the GGA+U method with  $U = 0.005$  eV. The x-axis is  $E - E_f$  (eV) and the y-axis is Density of states (states/eV).

$N$   
 $I$   $F . 4$   
 $(0 1 20)$   
 $2 < H < 5$ ,  
 $M H$   $F . 2( )$   $3. F$ ,  
 $F . 5$   
 BLFC  $P$   $F M$   
 $399$  O  $F .$   
 $5( ) . A$   $P F M$  BLFC  $F$

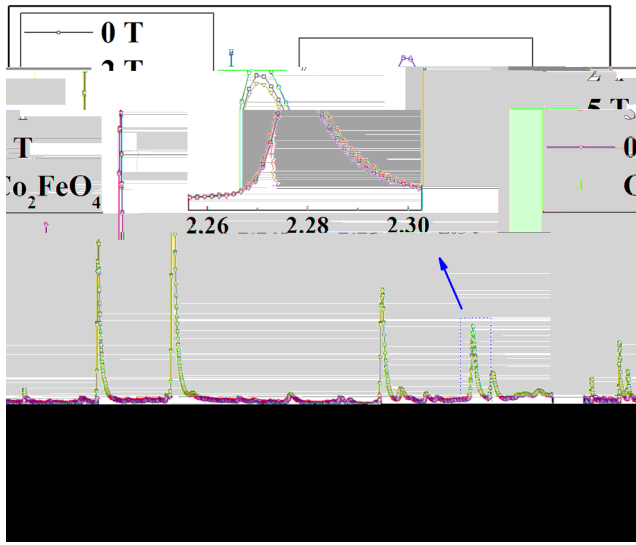


FIG. 4. XRD patterns of BLFC at 0 T, 2 T, and 5 T. The inset shows the magnified view of the 2.26–2.30 Å range.

Figure 4 shows the XRD patterns of BLFC at 0 T, 2 T, and 5 T. The patterns show a shift of the peaks towards lower angles with increasing magnetic field, indicating lattice expansion. The inset shows the magnified view of the 2.26–2.30 Å range, where a blue arrow points to a peak that shifts to lower angles as the magnetic field increases.

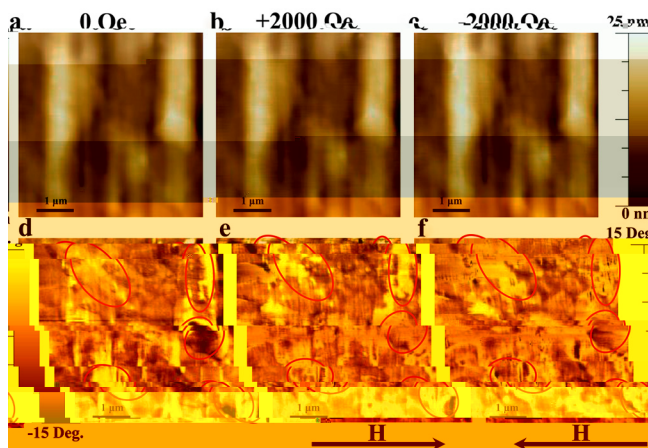


FIG. 5. TEM images of BLFC at different magnetic fields: (a) 0 Oe, (b) +2000 Oe, (c) -2000 Oe. (d) 0 Oe, (e) +2000 Oe, (f) -2000 Oe. The images show the morphology of the BLFC structure under different magnetic fields.

The structure of BLFC is shown in the schematic. The layers are FeO, Fe<sub>2</sub>O<sub>3</sub>, and FeO. The XRD patterns show a shift of the peaks towards lower angles with increasing magnetic field, indicating lattice expansion. The inset shows the magnified view of the 2.26–2.30 Å range, where a blue arrow points to a peak that shifts to lower angles as the magnetic field increases.

The structure of BLFC is shown in the schematic. The layers are FeO, Fe<sub>2</sub>O<sub>3</sub>, and FeO. The XRD patterns show a shift of the peaks towards lower angles with increasing magnetic field, indicating lattice expansion. The inset shows the magnified view of the 2.26–2.30 Å range, where a blue arrow points to a peak that shifts to lower angles as the magnetic field increases.

DATA AVAILABILITY

The data that support the findings of this study are available from the corresponding author upon request.

REFERENCES

1. E. J. Lee, N. D. M. J. F., *Nature* **442**, 759 (2006).
2. A. N. A., *Nature Materials* **6**, 21 (2007).
3. J. M. J. H., L. C., *Nature Materials* **23**, 1062 (2011).
4. L. F. H., O. C., J. B., J. L., C. H., H., O. G., D. C. L., H., K., A. J. B., *Advanced Functional Materials* **26**, 2111 (2016).
5. N. A. H., *Journal of Physical Chemistry B* **104**, 6694 (2000).
6. B. A., M., *Journal of Physical Chemistry B* **104**, 6694 (2000).
7. A., G. K., M. M. K., *Journal of Physical Chemistry B* **11**, 3335 (1999).
8. N. P., G. K., *Journal of Physical Chemistry B* **108**, 194 (2004).
9. L. K., M., A. A., N. D., N. P., M., E. P., D. J., *Journal of Physical Chemistry B* **96**, 2339 (2013).
10. L., J. M., G., K., A. M., L., C. J., C. N., H., *Journal of Physical Chemistry B* **45**, 14049 (2016).
11. J. F., *Nature Photonics* **5**, 72 (2013).
12. A. B., C. E., *Journal of Physical Chemistry B* **90**, 214109 (2014).
13. J. B. L., P. H., G. H., G. L., J. L., J. C., J. K. L., *Journal of Physical Chemistry Letters* **96**, 222903 (2010).
14. M., C., L., *Journal of Physical Chemistry Letters* **95**, 082901 (2009).
15. L., J., L., J. D., *Journal of Physical Chemistry Letters* **101**, 122402 (2012).

- <sup>16</sup>M. P. ... P. C. ..., M. B. ..., A. P. B. ..., J. P. H. ..., K. ..., L. K. ..., M. P. ..., C. ..., H. K. ..., A. J. B. ..., *J. A. P.* **112**, 073919 (2012).
- <sup>17</sup>J. L. ..., H. ..., M. J. ..., K. ..., P. ..., *J. A. P.* **102**, 104107 (2007).
- <sup>18</sup>M. G. C. ..., *Characterisation of Ferroelectric Bulk Materials and Thin Films* (..., 2014), ...2.
- <sup>19</sup>...L., K. ..., J. M. ..., G. ..., K. ..., C. J. ..., G. ..., H. ..., A. M. ..., J. C. ..., M. C. ..., I. A. ..., C. N. ..., C. J. ..., H. ..., *J. M. C. C.* **6**, 2733 (2018).
- <sup>20</sup>...K. ..., I. ..., G. ..., M. ..., C. J. ..., H. ..., *J. P. C.* **122**, 15733 (2018).
- <sup>21</sup>L. J. ..., F. L. ..., ..., *J. A. C.* **97**, 1 (2014).
- <sup>22</sup>H. ..., F. I. ..., G. ..., H. N. ..., H. ..., J. ..., G. ..., M. J. ..., *J. A. D.* **1**, 107 (2011).
- <sup>23</sup>J. ..., L. ..., L. ..., ..., J. D. ..., ..., *A. P. L.* **101**, 012402 (2012).
- <sup>24</sup>B. ..., J. ..., J. C. ..., L. ..., ..., J. D. ..., ..., *A. P. L.* **104**, 062413 (2014).
- <sup>25</sup>I. P. M. ..., N. B. ..., ..., **11**, 719 (2009).